AGU PUBLICATIONS

Geophysical Research Letters

RESEARCH LETTER
10.1002/2016GL070204

Key Points:
- OMI and adjoint modeling can constrain monthly anthropogenic SO_2 emissions
- Twenty percent emission reduction during the Beijing Olympic Games are made evident
- Posterior emissions improve monthly forecasts of surface and column SO_2

Correspondence to:
J. Wang,
jun-wang-1@uiowa.edu

Citation:
Wang, Y., J. Wang, X. Xu, D. K. Henze, Y. Wang, and Z. Qu (2016), A new approach for monthly updates of anthropogenic sulfur dioxide emissions from space: Application to China and implications for air quality forecasts, *Geophys. Res. Lett.*, *43*, 9931–9938 doi:10.1002/2016GL070204.

Received 27 JUN 2016
Accepted 31 AUG 2016
Accepted article online 3 SEP 2016
Published online 23 SEP 2016

A new approach for monthly updates of anthropogenic sulfur dioxide emissions from space: Application to China and implications for air quality forecasts

Yi Wang[1,2], Jun Wang[1,2], Xiaoguang Xu[1,2], Daven K. Henze[3], Yuxuan Wang[4,5], and Zhen Qu[3]

[1]Department of Earth and Atmospheric Sciences, University of Nebraska–Lincoln, Lincoln, Nebraska, USA, [2]Now at Center of Global and Regional Environmental Research, Department of Chemical and Biochemical Engineering, University of Iowa, Iowa City, Iowa, USA, [3]Department of Mechanical Engineering, University of Colorado Boulder, Boulder, Colorado, USA, [4]Department of Earth and Atmospheric Sciences, The University of Houston, Houston, Texas, USA, [5]Ministry of Education Key Laboratory for Earth System Modeling, Center for Earth System Science, Institute for Global Change Studies, Tsinghua University, Beijing, China

Abstract SO_2 emissions, the largest source of anthropogenic aerosols, can respond rapidly to economic and policy driven changes. However, bottom-up SO_2 inventories have inherent limitations owing to 24–48 months latency and lack of month-to-month variation in emissions (especially in developing countries). This study develops a new approach that integrates Ozone Monitoring Instrument (OMI) SO_2 satellite measurements and GEOS-Chem adjoint model simulations to constrain monthly anthropogenic SO_2 emissions. The approach's effectiveness is demonstrated for 14 months in East Asia; resultant posterior emissions not only capture a 20% SO_2 emission reduction in Beijing during the 2008 Olympic Games but also improve agreement between modeled and in situ surface measurements. Further analysis reveals that posterior emissions estimates, compared to the prior, lead to significant improvements in forecasting monthly surface and columnar SO_2. With the pending availability of geostationary measurements of tropospheric composition, we show that it may soon be possible to rapidly constrain SO_2 emissions and associated air quality predictions at fine spatiotemporal scales.

1. Introduction

Atmospheric sulfur dioxide (SO_2) is a pollutant emitted from anthropogenic activities (coal power plants, industry, and residential combustion) and natural sources (volcanoes and phytoplankton). Its reaction with H_2O and oxidants (H_2O_2 and O_3) in liquid phase leads to the formation of sulfuric acid (H_2SO_4) that can be dissolved into cloud water to form acid rain or be neutralized by NH_3 to form sulfate particles [*Wang et al.*, 2008a, 2008b]. Sulfate particles can further affect air quality and Earth's radiative energy budget through scattering of radiation and aerosol-cloud interactions [*Haywood and Boucher*, 2000]. In addition, higher-SO_2 conditions may enhance the formation of isoprene-derived secondary organic aerosol that also has significant influences on regional air quality and climate change [*Lin et al.*, 2013]. While the importance of SO_2 on air quality and climate change is recognized [*Myhre et al.*, 2013], a large range in estimates of anthropogenic SO_2 emissions exists. For example, the average, minimum, and maximum estimates of anthropogenic SO_2 emissions for year 2000 are, respectively, 55.2, 43.3, and 77.9 Tg S yr^{-1} globally and 11.7, 9.6, and 17.0 Tg S yr^{-1} over China [*Boucher et al.*, 2013]. Furthermore, those estimates are a result of the bottom-up approach that analyzes and integrates SO_2-related activity rates (of coal power plants, industry, and residential combustion) with SO_2 emission factors from various agencies and sources. Consequently, they have limitations in that they usually have a temporal lag of 2 to 3 years and can quickly become outdated [*Zhang et al.*, 2009b]. These limitations are further amplified at regional scales, such as in China which has experienced rapid economic development at the last two decades and is subject to implementation of emission control policy in various times [*Li et al.*, 2010].

Satellite observations that provide near-real-time information about atmospheric composition are useful constraints for detections and updates of emissions [*Streets et al.*, 2013]. *Xu et al.* [2013] used Moderate Resolution Imaging Spectroradiometer (MODIS) Aerosol Optical Depth (AOD) as constraints to estimate aerosol emissions (including SO_2) over China through an adjoint inverse modeling method. However, since SO_2 and aerosol particles co-exist in the atmosphere and sulfate is only one component of aerosol composition, the atmospheric SO_2 can be at least equally important as AOD in constraining SO_2 emissions. Indeed, the

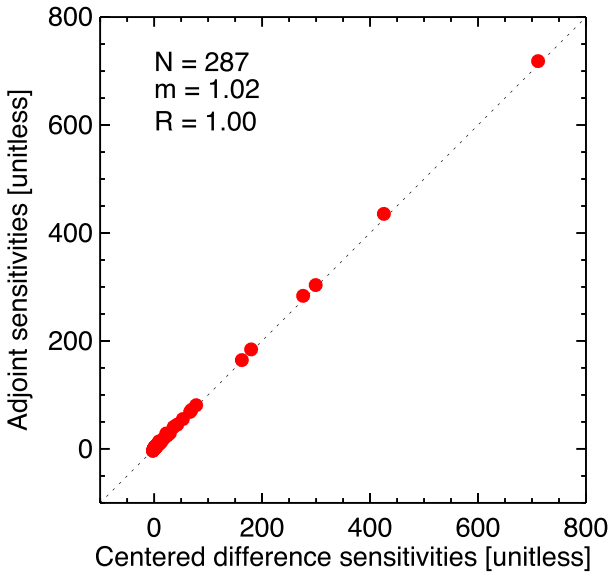

Figure 1. Validation of adjoint model sensitivities through comparison to centered finite difference results for a 3 day simulation. Shown here are the sensitivities of column cost function (penalty term is not included, and horizontal transport is turned off) with respect to anthropogenic SO_2 emission scale factors: the 1:1 line (dotted), the number of grid columns (*N*), the slope of linear regression (*m*), and correlation coefficient (*R*).

reduction of SO_2 emissions after implementing emission control policies since 2006 in China can be detected by Ozone Monitoring Instrument (OMI) [*Li et al.*, 2010; *Wang et al.*, 2015; *Zhang et al.*, 2009a]. *McLinden et al.* [2016] used OMI SO_2 observations to detect SO_2 sources that are not captured in conventional inventories. *Lee et al.* [2011] inferred a top-down SO_2 emission inventory through multiplying satellite-based SO_2 column amounts by the ratio between bottom-up SO_2 emissions and simulated SO_2 column amounts. *Fioletov et al.* [2013, 2015, 2016] approximately assumed linear relationship between reported emissions and total SO_2 molecules and used it to estimate large SO_2 point source, although the relationship should be nonlinear.

Here we present a new approach for using satellite observations and the GEOS-Chem adjoint model to constrain anthropogenic SO_2 emissions on a monthly basis, enabling reliable and rapid update of anthropogenic SO_2 emissions for both regional air quality forecast and climate studies. To account for the nonlinear relationship between SO_2 sources and atmospheric SO_2 abundance in the top-down emissions estimates, we develop the OMI SO_2 observation operator in the framework of the GEOS-Chem adjoint model [*Henze et al.*, 2007]. This study is different from the past studies in that (a) we develop a new approach to resolve month-to-month variation of anthropogenic SO_2 emissions and (b) we illustrate this approach with 14 months' regional air quality prediction and validate our method using both in situ SO_2 data and cross validation. We focus on China in this study as it has experienced rapid economic development at the last two decades and SO_2 loadings are high there.

2. GEOS-Chem Model, OMI, and In Situ SO_2 Data

GEOS-Chem is a global 3-D chemistry transport model driven by assimilated meteorological observations from the Goddard Earth Observing System (GEOS-5) at the NASA Goddard Global Modeling Assimilation Office [*Bey et al.*, 2001]. It has 47 vertical levels and a horizontal resolution of 2° latitude by 2.5° longitude in this study. Global anthropogenic emissions are from Emission Database for Global Atmospheric Research (http://edgar.jrc.ec.europa.eu/), and anthropogenic SO_2 emissions over China are replaced by Intercontinental Chemical Transport Experiment-Phase B (INTEX-B) emissions [*Zhang et al.*, 2009b]. The INTEX-B emission inventory was originally developed to support the INTEX-B field campaign in 2006 by using limited ancillary information for 2006 at that time and activity data extrapolated from available statistics for 2004 and 2005.

The new operational and science-grade total SO_2 slant column density level 3 daily products (http://disc.sci.gsfc.nasa.gov/Aura/data-holdings/OMI/1readme.omso2e.2015-02-12.pdf) from OMI are used to constrain anthropogenic SO_2 emissions over China. Compared with the previous operational OMI SO_2 band residual difference algorithm [*Krotkov et al.*, 2006], this new algorithm applies principal component analysis to the OMI spectra to extract a set of PCs to reduce retrieval interferences and, therefore, decreases the noise in SO_2 retrieval by a factor of 2 [*Li et al.*, 2013]. In situ observations of SO_2 at the Miyun (40°29′N, 116°46′E) site [*Y. Wang et al.*, 2010], which is about 100 km northeast from Beijing's urban center, are used for independent evaluation of the GEOS-Chem simulations.

3. GEOS-Chem Adjoint Model Development

The adjoint of the GEOS-Chem was developed specifically for inverse modeling of aerosol and aerosol precursor emissions [*Henze et al*., 2007]. It has the advantage of accurately and efficiently calculating sensitivities of a cost function with respect to model parameters such as scale factors for anthropogenic SO_2 emissions at every grid box. The inverse modeling process uses these sensitivities to optimize these emission scale factors. Previous top-down estimates of aerosol (and aerosol precursor) emissions have been conducted with GEOS-Chem [e.g., *Henze et al*., 2009; *Wang et al*., 2012; *Xu et al*., 2013; *Zhang et al*., 2014; *Zhu et al*., 2013] and other adjoint models [e.g., *Yumimoto and Takemura*, 2015].

Here we develop the OMI SO_2 observation operator for GEOS-Chem adjoint model, thereby enabling us, for the first time, to conduct top-down estimation of anthropogenic SO_2 emissions using their observations in an inverse modeling framework that accounts for the full sulfur chemistry and lifecycle in the atmosphere. The scaling factors of anthropogenic SO_2 emissions in each GEOS-Chem grid box ($\boldsymbol{\sigma}$) are optimized by minimizing the cost function, given by

$$J(\boldsymbol{\sigma}) = \frac{1}{2}\Sigma_{\Omega}[H(M(\boldsymbol{\sigma})) - \mathbf{c}_{obs}]^T \mathbf{S}_{\mathrm{obs}}^{-1}[H(M(\boldsymbol{\sigma})) - \mathbf{c}_{obs}] + \gamma\frac{1}{2}[\boldsymbol{\sigma} - \boldsymbol{\sigma}_a]^T \boldsymbol{S}_a^{-1}[\boldsymbol{\sigma} - \boldsymbol{\sigma}_a] \quad (1)$$

where $\boldsymbol{\sigma}$ is used to adjust elements of the vector of anthropogenic SO_2 emissions, $\mathbf{p}$, via application as scaling factors, $p = p_a e^{\sigma}$, $\mathbf{p_a}$ is prior anthropogenic SO_2 emission state vector, $\mathbf{c}_{\mathrm{obs}}$ is the vector of OMI slant column densities in four-dimension space Ω, M is the GEOS-Chem model, H is the observation operator which maps simulated SO_2 concentration to slant column SO_2 density, γ is a regularization parameter, $\mathbf{S}_{\mathrm{obs}}$ is observation error covariance matrix, $\boldsymbol{\sigma_a}$ is the prior estimate of $\boldsymbol{\sigma}$, and $\mathbf{S}_{\mathrm{a}}$ is the background error covariance for $\boldsymbol{\sigma_a}$. The sensitivities of the cost function with respect to $\boldsymbol{\sigma}$ calculated from GEOS-Chem adjoint are used to minimize the cost function iteratively with the quasi-Newton L-BFGS-B algorithm [*Byrd et al*., 1995].

In the development of OMI SO_2 observation operator H, the vertical columnar SO_2 from GEOS-Chem is first converted to the slant column by applying a local air mass factor (AMF) that corresponds to the OMI observation. Local AMF is calculated according to equation (2)

$$\mathrm{AMF} = \mathrm{AMF}_G \int_0^{\infty} w(z) S_z(z) dz \quad (2)$$

where AMF_G is the geometric air mass factor, $w(z)$ are scattering weights calculated using the VLIDORT radiative transfer code [*Spurr*, 2006], and $S_z(z)$ is SO_2 shape factor from GEOS-Chem simulation. *Palmer et al*. [2001] and *Lee et al*. [2009] give details of derivation and application of this AMF calculation method. The accuracy of the adjoint sensitivities is evaluated with finite difference sensitivities. Figure 1 shows that the sensitivities of column cost function with respect to anthropogenic SO_2 emission scale factors from adjoint model agrees quite well with that of finite difference method [*Henze et al*., 2007] in terms of linear correlation coefficient (1.00) and linear regression slope (1.02), hence verifying the addition of our new observation operator to the adjoint model.

In inverse modeling, balancing the contribution of total prediction error and penalty error in the cost function is a key aspect. Due to the lack of rigorous statistical information on the error covariance of the emissions, we assume the error is uncorrelated and use the L-curve method [*Hansen*, 1998] to determine a regularization parameter, γ. The relative errors of SO_2 emissions are taken to be 50%. Observation errors are also considered as uncorrelated and set as 0.25 DU which is the standard deviation of OMI SO_2 over the presumably SO_2-free Pacific Ocean (http://disc.sci.gsfc.nasa.gov/Aura/data-holdings/OMI/documents/v003/omso2readme-v120-20140926.pdf).

4. Experiments and Results

We conduct a series of numerical experiments to evaluate the new approach to constraining anthropogenic SO_2 emissions with OMI SO_2 observations using the GEOS-Chem adjoint model. First, the method is applied to April and August 2008 over East Asia. The real anthropogenic SO_2 emissions over Beijing and its surrounding areas in August 2008 should be smaller than those in April 2008 as special emission controls were implemented in August 2008 over this region for the 29th Olympic Games. Thus, evaluating the results between the two months provides a first check of the effectiveness of the new approach. This is then followed by applying our method for 1 year (December 2008 to November 2009) to evaluate the potential of our

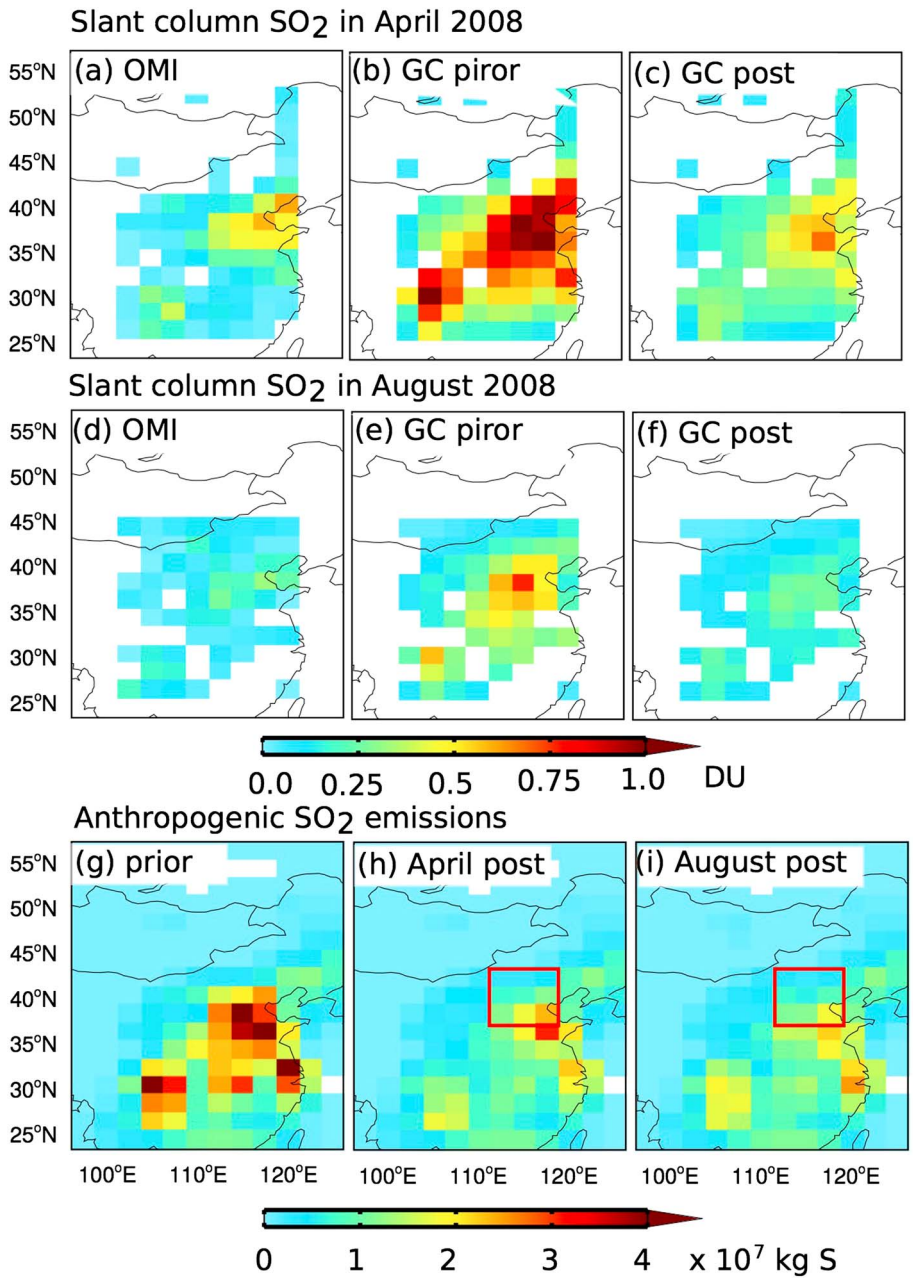

Figure 2. Slant column SO_2 and anthropogenic SO_2 emissions. (a–c) The slant column SO_2 from OMI, prior, and posterior GEOS-Chem simulation for April 2008, respectively. (d–f) Same as Figures 2a–2c but for August 2008. (g–i) Prior anthropogenic SO_2 emissions and posterior anthropogenic SO_2 emissions for April and August 2008, respectively. The red box represents the region where strong emission controls occurred in August 2008.

approach for air quality forecasts and chemical composition reanalysis. Evaluations are conducted to (a) compare the posterior simulation with in situ surface SO_2 data and (b) apply the posterior anthropogenic SO_2 emissions from the previous month (e.g., January or February of 2009) to forecast the air quality in the current month of interest (e.g., February or March of 2009) and evaluate the forecasts with OMI slant column SO_2 and in situ SO_2 data. Hence, there are 14 months of results (including April and August 2008) to be evaluated in (a) and only 13 months (August 2008 is not included due to special emission control) of results to be evaluated in (b). Evaluation from (b) can reveal the practical applications for this approach for operational air quality forecast.

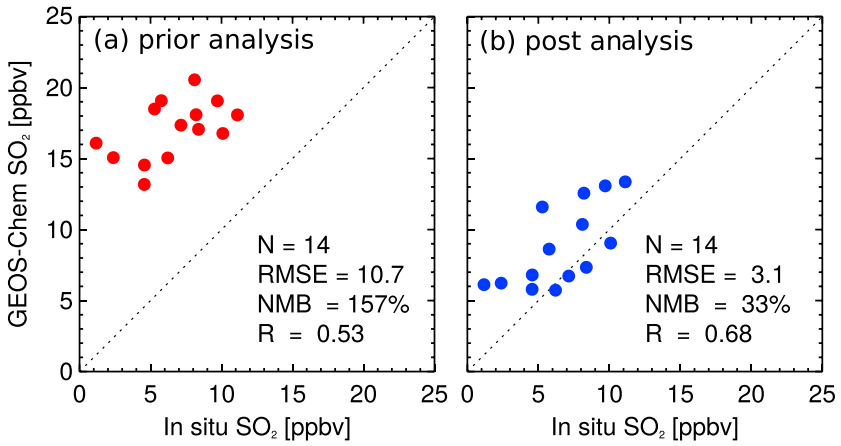

Figure 3. Scatter plot of GEOS-Chem monthly mean surface SO_2 simulated with (a) prior emission and (b) posterior emission versus in situ observations in Miyun for monthly cases of April 2008, August 2008, and December 2008 to November 2009. The number of months (*N*), root-mean-square error (RMSE), normalized mean bias (NMB), and linear correlation coefficient (*R*) are also shown.

4.1. Results for April and August 2008

During 8–24 August 2008 the 29th Olympic Games were held in Beijing, and emission control policies were implemented in Beijing and its surrounding regions. Vehicles were restricted, production was limited or even stopped at heavily polluting factories in Beijing, and power plants located in surrounding regions were required to use cleaner desulfurized coal from 20 July to 20 September [*Wang et al*., 2009]. Thus, significant reduction of SO_2 emissions occurred in Beijing and its surrounding regions in August 2008. We consider April 2008 to be a representative of a month with normal emissions, as there was no special emission control during that month. Figures 2b and 2e show simulated prior slant column SO_2 in April and August. Although the same SO_2 emission inventory is used in each of these months, the slant column SO_2 in August is much smaller than in April due to larger wet deposition in August. Inverse modeling leads to improved agreement of simulated slant column SO_2 compared to OMI observations in April (Figures 2a–2c) and August (Figures 2d–2f). Figures 2g–2i show the geographic distribution of the prior and posterior anthropogenic SO_2 emissions for April and August 2008. The anthropogenic SO_2 emission in April 2008 over China decrease from 1300 Gg S in the prior INTEX-B inventory to 843 Gg S (~35.2% decrease) in the posterior which is in good agreement with the 865 Gg S (~33.5% decrease) retrieved through integration of MODIS AOD and GEOS-Chem adjoint model [*Xu et al*., 2013], and the spatial linear correlation coefficient of the two posterior emission inventories is 0.97. These consistencies provide a basis for simultaneously using both SO_2 and AOD measurements to constrain SO_2 emissions for future studies. A decrease trend of China SO_2 emissions from 2006 to 2008 has been found based on bottom-up estimates by *Lu et al*. [2011] from 17 to 16 (~5.9% decrease) Tg S. The reduction of 35.2% in April can be interpreted by the joint contribution of a decrease trend and a possible overestimation in INTEX-B bottom-up inventory [*Xu et al*., 2013]. Compared to the prior anthropogenic SO_2 emissions, posterior anthropogenic SO_2 emissions for both April and August decrease, which is consistent with the SO_2 emissions decreasing trend from 2006 to 2008 [*Lu et al*., 2011]. Besides, the distribution of posterior anthropogenic SO_2 emission captures a ~20% decline of SO_2 emissions in Beijing and its surrounding regions (red box in Figure 2) from 89 Gg S for April to 71 Gg S for August. *S. Wang et al*. [2010] estimated with a bottom-up method that SO_2 emissions during the Olympic Games in Beijing were 41% lower than in June 2008. The lower reduction in our estimate is likely due to our model horizontal model resolution of 2° latitude by 2.5° longitude, which covers an area larger than the Beijing metropolitan area, and that stronger emission control occurred in Beijing than its surrounding regions during the Olympic Games.

4.2. Evaluation With In Situ SO_2

To evaluate the inversion results, we also use in situ SO_2 data from a site in Miyun to evaluate monthly mean surface SO_2 concentration simulated from GEOS-Chem using the prior and posterior emissions. As shown in Figure 3, the posterior estimates exhibit better agreement with SO_2 at the Miyun site than the prior estimates:

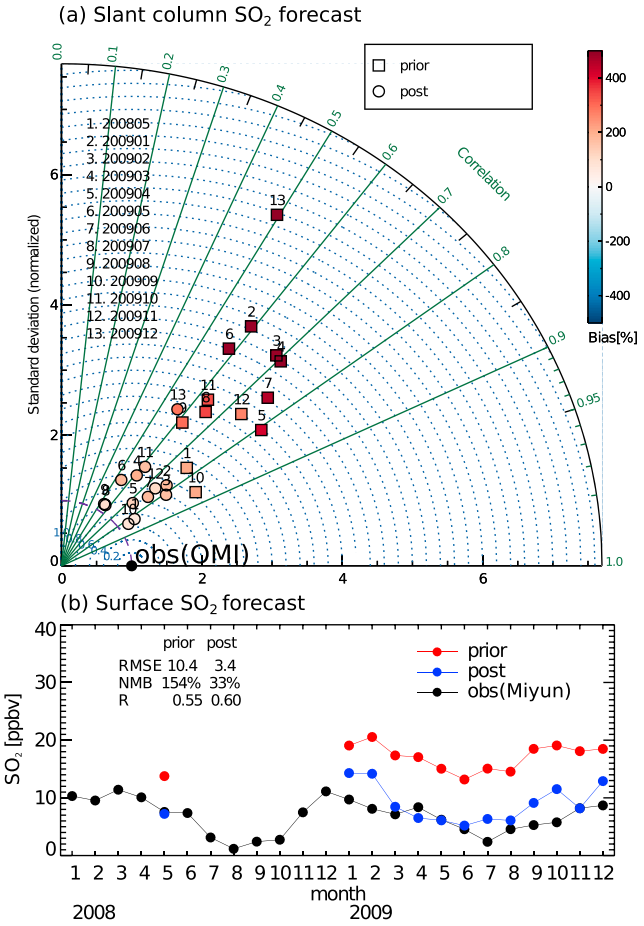

Figure 4. Comparisons of GEOS-Chem SO_2 forecast using INTEX-B emission (prior forecast runs) and posterior emission of last month (posterior forecast runs) to observations during May 2008 and January to December 2009. (a) Taylor diagram of evaluating GEOS-Chem slant column SO_2 from prior forecast runs (squares) and posterior forecast runs (circles) against OMI slant column SO_2 observations (obs point). The color on each point indicates the normalized mean bias. (b) Time series of monthly mean surface SO_2 sampled at Miyun site from prior forecast runs (red) and posterior forecast runs (blue) and in situ observation (black). The root-mean-square error (RMSE), normalized mean bias (NMB), and correlation coefficient (*R*) are also shown.

the linear correlation coefficient (*R*) increases from 0.53 for prior analysis to 0.68 for posterior analysis; normalized mean bias (NMB) decreases from 157% to 33%; and root-mean-square error (RMSE) reduces from 10.7 to 3.1 (Figures 3a and 3b).

4.3. Air Quality Forecast Applications

The application of using posterior anthropogenic SO_2 emissions from the previous month to forecast SO_2 concentrations in a subsequent month is shown in Figure 4. Figure 4 a is a Taylor diagram which evaluates the slant column SO_2 from posterior forecasts (use posterior anthropogenic SO_2 emission of previous month) and prior forecasts (use INTEX-B anthropogenic SO_2 emission) with OMI slant column SO_2. It is clear from the Taylor diagram that posterior forecasts (circular points) are generally closer than the prior forecasts (square points) to the OMI slant column SO_2 reference point (obs point) and to the unity curve of normalized standard deviation. In addition, posterior forecasts exhibit remarkably decreased bias ranging from 127% to 342% in the 13 monthly cases. To further show the ability of the new approach for air quality forecast, we use in situ observations at the Miyun site to assess model surface SO_2 forecasts in Figure 4b. Although both prior and posterior forecasts capture winter enhancement and summer decline of SO_2, NMB and RMSE decrease, respectively, from 154% and 10.5 in prior forecasts to 33% and 3.4 in posterior forecasts, while linear correlation coefficient increases from 0.55 to 0.60. Both evaluations indicate a notable improvement (reduction of bias more than by 100%) in the application of posterior anthropogenic SO_2 emission for air quality forecasting regardless of the observational data used for assessments.

5. Summary and Discussions

We develop a method that assimilates OMI SO_2 observations using the GEOS-Chem adjoint model for timely updates to anthropogenic SO_2 emissions and for improved air quality forecasts. The approach and application are tested on a monthly basis over China. Our approach captures a 20% reduction of anthropogenic emissions occurred in Beijing and its surrounding regions in August 2008 due to the Olympic Games as compared to April 2008. Additionally, GEOS-Chem surface SO_2 data simulated with posterior emissions exhibit a better agreement with in situ observations than the counterparts obtained using prior emissions; the linear correlation coefficient increases by 0.15 and NMB and RMSE both decrease by 124% and 7.6, respectively. The

posterior anthropogenic SO_2 emission in each month are applied to the subsequent month for SO_2 forecasts, which yields better agreement (reduction of bias more than by 100%) between forecasted and (OMI and in situ) observed SO_2 as compared to results that use the prior emission in GEOS-Chem. OMI SO_2 observations are available at near real time; thus, we can get timely update of SO_2 emission inventory through this approach and provide it to air quality forecast community. Considering that sulfate-nitrate-ammonium aerosol mass concentrations are most sensitive to SO_2 emissions among nitrogen oxides (NO_x), SO_2, and ammonia (NH_3) emissions during most of the year [*Kharol et al*., 2013; *Wang et al*., 2013], and SO_2 emissions have important influence on surface $PM_{2.5}$ (e.g., SO_2 emissions contribute 14% to wintertime surface $PM_{2.5}$ in Beijing [*Lin et al*., 2015]), our approach for improving SO_2 forecasts would thus likely result in significant improvements of $PM_{2.5}$ air quality forecasts. Furthermore, the application of our approach to the whole record of OMI SO_2 data since 2006 is now ongoing, and the resultant monthly SO_2 emission will be made publically available for chemistry transport modeling community that has a high interest in conducting reanalysis of atmospheric composition.

Although this study presents, for the first time, integration of satellite SO_2 observations and GEOS-Chem adjoint model to constrain anthropogenic SO_2 emissions, we expect to assimilate observational AOD, SO_2, and NO_2 simultaneously to constrain SO_2 and NO_2 emissions in future research. Emissions of SO_2 and NO_2 can only be fully constrained with their satellite-based counterpart products and AOD, because they contribute both to the formation of sulfate and nitrate in the particle phase and to the atmospheric SO_2 and NO_2 in the gas phase, respectively. Thus, using either SO_2 or NO_2 alone can only provide partial constraint to the emission of the corresponding trace gases. Together with our past study that presented the ability of using MODIS AOD to invert species-specific aerosol emissions [*Xu et al*., 2013], this study supports the concept of using multisensor data (MODIS AOD, OMI SO_2 and NO_2) to constrain emissions of both aerosol primary and precursor emissions in near future. While the method developed in this study is illustrated with the GEOS-Chem adjoint model at a relatively coarse resolution of $2° \times 2.5°$, it can be applied to the GEOS-Chem adjoint at finer resolution of $0.5° \times 0.666°$ or even $0.25° \times 0.3125°$ (albeit the needs of more computational power), thereby working in tandem with future high-resolution geostationary instruments to characterize local-to-regional aerosol sources and precursors. With the launch of Geostationary Environment Monitoring Spectrometer (GEMS), Sentinel-4, Tropospheric Emissions: Monitoring of Pollution (TEMPO), and Geostationary Operational Environmental Satellite-R series (GOES-R) that will measure AOD, SO_2, and NO_2 at the high temporal resolution (<1 h) and spatial resolution (<4 km) in the coming decade, it is foreseeable that the bottom-up emission inventory can be updated timely to provide unprecedented opportunity to improve the air quality analysis and forecast. Evaluation of such analysis and forecast would require publically accessible observation data of air pollutants from more ground-based observation site, especially in developing countries.

Acknowledgments
This work is supported by NASA Atmospheric Chemistry Modeling and Analysis Program (NNX13AK86G) managed by Richard S. Eckman, NASA Radiation Sciences Program managed by Hal B. Maring, NASA Aura Science managed by Kenneth Jucks, and NASA Applied Science program managed by John Haynes. Data shown in the paper can be obtained from the corresponding author through e-mail (jwangjun@gmail.com).

References

Bey, I., D. J. Jacob, R. M. Yantosca, J. A. Logan, B. D. Field, A. M. Fiore, Q. Li, H. Y. Liu, L. J. Mickley, and M. G. Schultz (2001), Global modeling of tropospheric chemistry with assimilated meteorology: Model description and evaluation, *J. Geophys. Res.*, *106*(D19), 23,073–23,095, doi:10.1029/2001JD000807.

Boucher, O., et al. (2013), Clouds and aerosols, in *Climate Change 2013: The Physical Science Basis. Contribution of Working Group I to the Fifth Assessment Report of the Intergovernmental Panel on Climate Change*, edited by T. F. Stocker et al., pp. 571–658, Cambridge Univ. Press, Cambridge, U. K. and New York.

Byrd, R., P. Lu, J. Nocedal, and C. Zhu (1995), A limited memory algorithm for bound constrained optimization, *SIAM J. Sci. Comput.*, *16*(5), 1190–1208, doi:10.1137/0916069.

Fioletov, V. E., et al. (2013), Application of OMI, SCIAMACHY, and GOME-2 satellite SO_2 retrievals for detection of large emission sources, *J. Geophys. Res. Atmos.*, *118*, 11,399–11,418, doi:10.1002/jgrd.50826.

Fioletov, V. E., C. A. McLinden, N. Krotkov, and C. Li (2015), Lifetimes and emissions of SO_2 from point sources estimated from OMI, *Geophys. Res. Lett.*, *42*, 1969–1976, doi:10.1002/2015GL063148.

Fioletov, V. E., C. A. McLinden, N. Krotkov, C. Li, J. Joiner, N. Theys, S. Carn, and M. D. Moran (2016), A global catalogue of large SO_2 sources and emissions derived from the Ozone Monitoring Instrument, *Atmos. Chem. Phys. Discuss.*, *2016*, 1–45, doi:10.5194/acp-2016-417.

Hansen, P. C. (1998), *Rank-Deficient and Discrete Ill-Posed Problems: Numerical Aspects of Linear Inversion*, Society for Industrial Mathematics, Philadelphia, Pennsylvania.

Haywood, J., and O. Boucher (2000), Estimates of the direct and indirect radiative forcing due to tropospheric aerosols: A review, *Rev. Geophys.*, *38*(4), 513–543, doi:10.1029/1999RG000078.

Henze, D. K., A. Hakami, and J. H. Seinfeld (2007), Development of the adjoint of GEOS-Chem, *Atmos. Chem. Phys.*, *7*(9), 2413–2433, doi:10.5194/acp-7-2413-2007.

Henze, D. K., J. H. Seinfeld, and D. T. Shindell (2009), Inverse modeling and mapping US air quality influences of inorganic $PM_{2.5}$ precursor emissions using the adjoint of GEOS-Chem, *Atmos. Chem. Phys.*, *9*(16), 5877–5903, doi:10.5194/acp-9-5877-2009.

Kharol, S. K., R. V. Martin, S. Philip, S. Vogel, D. K. Henze, D. Chen, Y. Wang, Q. Zhang, and C. L. Heald (2013), Persistent sensitivity of Asian aerosol to emissions of nitrogen oxides, *Geophys. Res. Lett.*, *40*, 1021–1026, doi:10.1002/grl.50234.

Krotkov, N. A., S. A. Carn, A. J. Krueger, P. K. Bhartia, and Y. Kai (2006), Band residual difference algorithm for retrieval of SO_2 from the aura ozone monitoring instrument (OMI), *IEEE Trans. Geosci. Remote Sens.*, *44*(5), 1259–1266, doi:10.1109/TGRS.2005.861932.

Lee, C., R. V. Martin, A. van Donkelaar, G. O'Byrne, N. Krotkov, A. Richter, L. G. Huey, and J. S. Holloway (2009), Retrieval of vertical columns of sulfur dioxide from SCIAMACHY and OMI: Air mass factor algorithm development, validation, and error analysis, *J. Geophys. Res.*, *114*, D22303, doi:10.1029/2009JD012123.

Lee, C., R. V. Martin, A. van Donkelaar, H. Lee, R. R. Dickerson, J. C. Hains, N. Krotkov, A. Richter, K. Vinnikov, and J. J. Schwab (2011), SO_2 emissions and lifetimes: Estimates from inverse modeling using in situ and global, space-based (SCIAMACHY and OMI) observations, *J. Geophys. Res.*, *116*, D06304, doi:10.1029/2010JD014758.

Li, C., Q. Zhang, N. A. Krotkov, D. G. Streets, K. He, S.-C. Tsay, and J. F. Gleason (2010), Recent large reduction in sulfur dioxide emissions from Chinese power plants observed by the Ozone Monitoring Instrument, *Geophys. Res. Lett.*, *37*, L08807, doi:10.1029/2010GL042594.

Li, C., J. Joiner, N. A. Krotkov, and P. K. Bhartia (2013), A fast and sensitive new satellite SO_2 retrieval algorithm based on principal component analysis: Application to the ozone monitoring instrument, *Geophys. Res. Lett.*, *40*, 6314–6318, doi:10.1002/2013GL058134.

Lin, Y. H., E. M. Knipping, E. S. Edgerton, S. L. Shaw, and J. D. Surratt (2013), Investigating the influences of SO_2 and NH_3 levels on isoprene-derived secondary organic aerosol formation using conditional sampling approaches, *Atmos. Chem. Phys.*, *13*(16), 8457–8470, doi:10.5194/acp-13-8457-2013.

Lin, Z., L. Licheng, Z. Yuanhong, G. Sunling, Z. Xiaoye, K. H. Daven, L. C. Shannon, F. Tzung-May, Z. Qiang, and W. Yuxuan (2015), Source attribution of particulate matter pollution over North China with the adjoint method, *Environ. Res. Lett.*, *10*(8), 084011.

Lu, Z., Q. Zhang, and D. G. Streets (2011), Sulfur dioxide and primary carbonaceous aerosol emissions in China and India, 1996–2010, *Atmos. Chem. Phys.*, *11*(18), 9839–9864, doi:10.5194/acp-11-9839-2011.

McLinden, C. A., V. Fioletov, M. W. Shephard, N. Krotkov, C. Li, R. V. Martin, M. D. Moran, and J. Joiner (2016), Space-based detection of missing sulfur dioxide sources of global air pollution, *Nat. Geosci.*, *9*, 496–500, doi:10.1038/ngeo2724.

Myhre, G., et al. (2013), Anthropogenic and natural radiative forcing, in *Climate Change 2013: The Physical Science Basis. Contribution of Working Group I to the Fifth Assessment Report of the Intergovernmental Panel on Climate Change*, edited by T. F. Stocker et al., pp. 659–740, Cambridge Univ. Press, Cambridge, U. K. and New York.

Palmer, P. I., D. J. Jacob, K. Chance, R. V. Martin, R. J. D. Spurr, T. P. Kurosu, I. Bey, R. Yantosca, A. Fiore, and Q. Li (2001), Air mass factor formulation for spectroscopic measurements from satellites: Application to formaldehyde retrievals from the Global Ozone Monitoring Experiment, *J. Geophys. Res.*, *106*(D13), 14,539–14,550, doi:10.1029/2000JD900772.

Spurr, R. J. D. (2006), VLIDORT: A linearized pseudo-spherical vector discrete ordinate radiative transfer code for forward model and retrieval studies in multilayer multiple scattering media, *J. Quant. Spectros. Radiat. Transfer*, *102*(2), 316–342, doi:10.1016/j.jqsrt.2006.05.005.

Streets, D. G., et al. (2013), Emissions estimation from satellite retrievals: A review of current capability, *Atmos. Environ.*, *77*, 1011–1042, doi:10.1016/j.atmosenv.2013.05.051.

Wang, J., D. J. Jacob, and S. T. Martin (2008a), Sensitivity of sulfate direct climate forcing to the hysteresis of particle phase transitions, *J. Geophys. Res.*, *113*, D11207, doi:10.1029/2007JD009368.

Wang, J., A. A. Hoffmann, R. J. Park, D. J. Jacob, and S. T. Martin (2008b), Global distribution of solid and aqueous sulfate aerosols: Effect of the hysteresis of particle phase transitions, *J. Geophys. Res.*, *113*, D11206, doi:10.1029/2007JD009367.

Wang, J., X. Xu, D. K. Henze, J. Zeng, Q. Ji, S.-C. Tsay, and J. Huang (2012), Top-down estimate of dust emissions through integration of MODIS and MISR aerosol retrievals with the GEOS-Chem adjoint model, *Geophys. Res. Lett.*, *39*, L08802, doi:10.1029/2012GL051136.

Wang, M., T. Zhu, J. Zheng, R. Y. Zhang, S. Q. Zhang, X. X. Xie, Y. Q. Han, and Y. Li (2009), Use of a mobile laboratory to evaluate changes in on-road air pollutants during the Beijing 2008 Summer Olympics, *Atmos. Chem. Phys.*, *9*(21), 8247–8263, doi:10.5194/acp-9-8247-2009.

Wang, S., M. Zhao, J. Xing, Y. Wu, Y. Zhou, Y. Lei, K. He, L. Fu, and J. Hao (2010), Quantifying the air pollutants emission reduction during the 2008 Olympic Games in Beijing, *Environ. Sci. Technol.*, *44*(7), 2490–2496, doi:10.1021/es9028167.

Wang, S., Q. Zhang, R. V. Martin, S. Philip, F. Liu, M. Li, X. Jiang, and K. He (2015), Satellite measurements oversee China's sulfur dioxide emission reductions from coal-fired power plants, *Environ. Res. Lett.*, *10*(11), 114015.

Wang, Y., J. W. Munger, S. Xu, M. B. McElroy, J. Hao, C. P. Nielsen, and H. Ma (2010), CO_2 and its correlation with CO at a rural site near Beijing: Implications for combustion efficiency in China, *Atmos. Chem. Phys.*, *10*(18), 8881–8897, doi:10.5194/acp-10-8881-2010.

Wang, Y., Q. Q. Zhang, K. He, Q. Zhang, and L. Chai (2013), Sulfate-nitrate-ammonium aerosols over China: Response to 2000–2015 emission changes of sulfur dioxide, nitrogen oxides, and ammonia, *Atmos. Chem. Phys.*, *13*(5), 2635–2652, doi:10.5194/acp-13-2635-2013.

Xu, X., J. Wang, D. K. Henze, W. Qu, and M. Kopacz (2013), Constraints on aerosol sources using GEOS-Chem adjoint and MODIS radiances, and evaluation with multisensor (OMI, MISR) data, *J. Geophys. Res. Atmos.*, *118*, 6396–6413, doi:10.1002/jgrd.50515.

Yumimoto, K., and T. Takemura (2015), Long-term inverse modeling of Asian dust: Interannual variations of its emission, transport, deposition, and radiative forcing, *J. Geophys. Res. Atmos.*, *120*, 1582–1607, doi:10.1002/2014JD022390.

Zhang, L., D. K. Henze, G. A. Grell, G. R. Carmichael, N. Bousserez, Q. Zhang, and J. Cao (2014), Constraining black carbon aerosol over Southeast Asia using OMI aerosol absorption optical depth and the adjoint of GEOS-Chem, *Atmos. Chem. Phys. Discuss.*, *14*(21), 28,385–28,452, doi:10.5194/acpd-14-28385-2014.

Zhang, Q., D. G. Streets, and K. He (2009a), Satellite observations of recent power plant construction in Inner Mongolia, China, *Geophys. Res. Lett.*, *36*, L15809, doi:10.1029/2009GL038984.

Zhang, Q., et al. (2009b), Asian emissions in 2006 for the NASA INTEX-B mission, *Atmos. Chem. Phys.*, *9*(14), 5131–5153, doi:10.5194/acp-9-5131-2009.

Zhu, L., D. K. Henze, K. E. Cady-Pereira, M. W. Shephard, M. Luo, R. W. Pinder, J. O. Bash, and G. R. Jeong (2013), Constraining U.S. ammonia emissions using TES remote sensing observations and the GEOS-Chem adjoint model, *J. Geophys. Res. Atmos.*, *118*, 3355–3368, doi:10.1002/jgrd.50166.